Uniaxial displacement controlled loading test of shape memory NiTi alloys

Xuyang Chang, Karine-Lavernhe Taillard, Olivier Hubert

UNI-AXIAL DISPLACEMENT CONTROLLED LOADING TEST OF SHAPE MEMORY NITI ALLOYS

Xuyang Chang [a], Karine-Lavernhe Taillard [a], Olivier Hubert [a]

[a] LMT (ENS Paris-Saclay / CNRS / Université Paris-Saclay) 61, Avenue du Président Wilson F-94235 CACHAN Cedex, email : chang@lmt.ens-cachan.fr ,

Mots-clefs: Displacement controlled loading #1, Shape memory alloy (SMA) #2, Digital images correlation (DIC) #3 .

1 Introduction

Shape Memory Alloys (SMA) are a class of smart materials that undergoes an austenite-martensite solid- solid, isochoric, diffusion-less, 1st order phase transformation which confers its pseudo-elasticity (PE) and/or shape memory effect (SME) [1] [2]. Phase transformation can be induced either by stress or temperature changes, thus indicating a strong thermomechanical coupled behavior. In industrial applications, SMA structures are on the other hand subjected to complex service conditions, such as large deformations, thermomechanical, multiaxial, and cyclic loading. Consequently, a robust multiphysic 3D modeling of phenomena governing theses behaviors is needed [3]. In order to construct a 3D thermal-mechanical coupled model, a campaign of 1D and 2D thermal-mechanical loading test is needed to identify the parameters. The loading test in uni-axial condition is especially addressed in this communication.

Displacement-controlled uniaxial tensile test experiments are performed over a small 1D NiTi strip to concentrate the stress level in the central zone and improve the heat exchange efficiency from the sample (due to phase transformation) to environment. Regularized Digital Images Correlation (R-DIC) technique is used to capture the temporal evolution of the displacement and strain fields[4]. The influence of the presence of localization bands over the macroscopic stress-strain curve is firstly investigated. The local strain stress curve inside and outside the band are then compared to evaluate the homogeneity/heterogeneity of the strain field during the test and to conclude about the relevancy of this test.

2 Experimental Setups

2.1 1D strip

A textured poly-crystalline NiTi specimen is considered. The 1D strip specimen is a thin plate with a thickness $e = 0.3\,\mathrm{mm}$ in the zone of interest with a rectangular shape : length =$10\,\mathrm{mm}$, width = $3\,\mathrm{mm}$. This specific design permits to avoid local heat accumulation due to phase transformation during the loading process. In its zone of interest (ZOI), the sample's surface is covered by a black and white speckle pattern made of double internal mix airbrush (see Figure 1.a). The presence of the black and white pattern increases the gray level contrast inside the image. This condition is essential to conduct an accurate DIC analysis.

2.2 Loading set-up [5]

The machine used to apply the mechanical loading is shown below (Figure 1.b). This mini loading machine has 4 independent motors, that permit to apply any proportional or non-proportional displacement-controlled loading. Two cold-light sources generate a homogeneous lighting condition over the surface of the specimen. A camera is placed above perpendicular to the surface of the specimen to capture the image sequence at a given acquisition frequency.

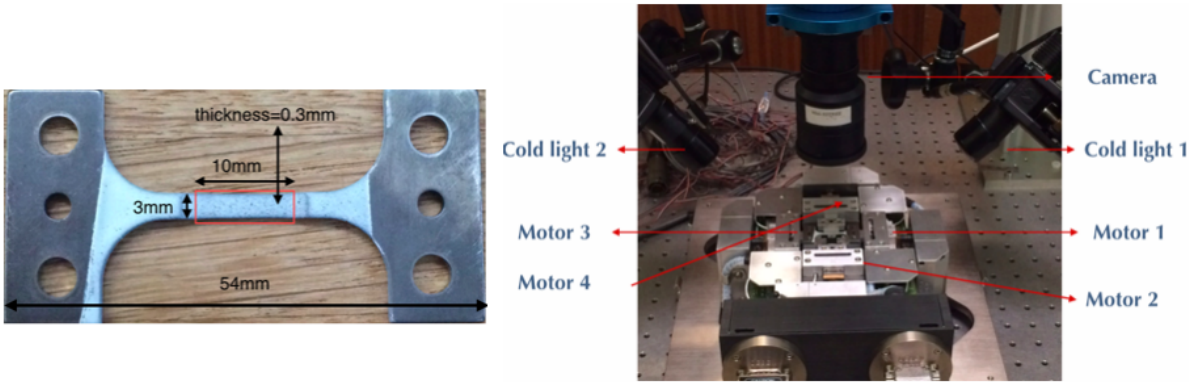

Figure 1: 1.a 1D strip covered with a black and white speckle pattern 1.b Experimental setup

3 1D test performed at 300K

Quasi-static displacement loading is applied to 1D NiTi strip at room temperature ($T = 300K$). Axial strain field is calculated by R-DIC analysis between reference image and deformed image. Axial tensile force is measured by the force cells of the machine.The average true axial strain and stress are calculated as follows:

$$\epsilon = \frac{1}{N}\sum \epsilon^i \tag{1}$$

$$\sigma = \frac{F}{s_0}(1+\epsilon) \tag{2}$$

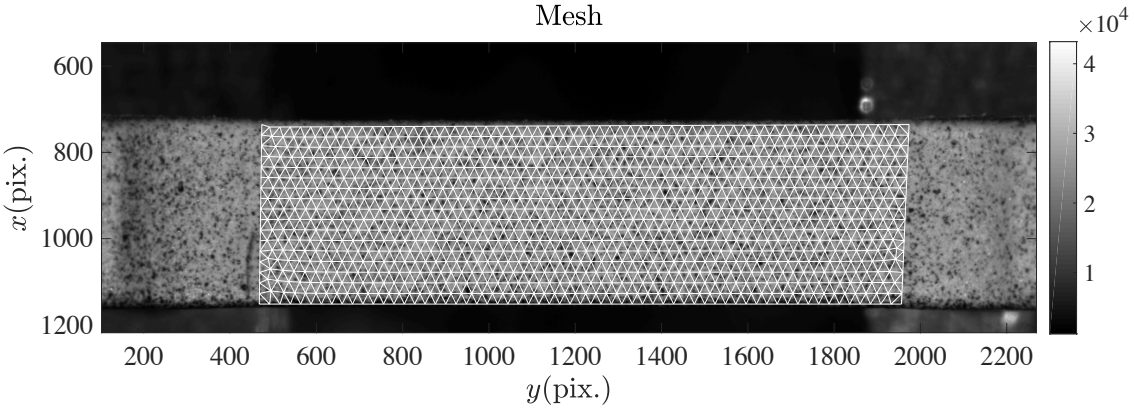

Figure 2: Chosen gauge in the centre zone

As we could see in Equation 2 and in Figure 2, the axial strain value is an average value of axial strains over all elements inside the chosen gauge of DIC. Average stress-strain behavior is plotted in Figure 3. Some remarkable points are highlighted and discussed below.

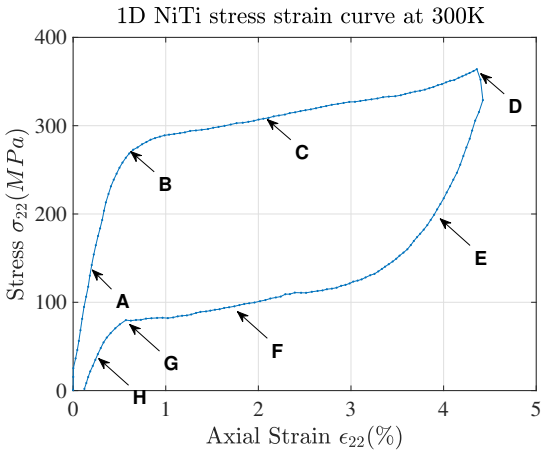

Figure 3: NiTi strip 1D stress strain curve at 300K

4 Localization Bands

4.1 Evolution of the strain field

The strain field evolution is showed in Figure 4 and Figure 5 in eight steps. The eight steps correspond to points A to H reported Figure 3;

Point A : In the elastic regime, stress-axial strain behavior is linear and reversible, strain field remains small and its distribution is nearly homogeneous;

Point B : Transformation begins, the localization band appears on the left side of the center zone;

Point C : Transformation regime continues, with increasing stress level, the localization band enlarges.

Point D : Beginning of unloading : the maximum average strain is obtained;

Point E : 1st elastic unloading;

Point F : Disappearance of strain band, leading approximately to the same deformation field than point C for a much lower stress level. This is a clear highlighting of stress/strain hysteresis.;

Point G : Localization bands nearly disappear;

Point H : 2nd elastic unloading regime, strain field returns to a nearly homogeneous state ;

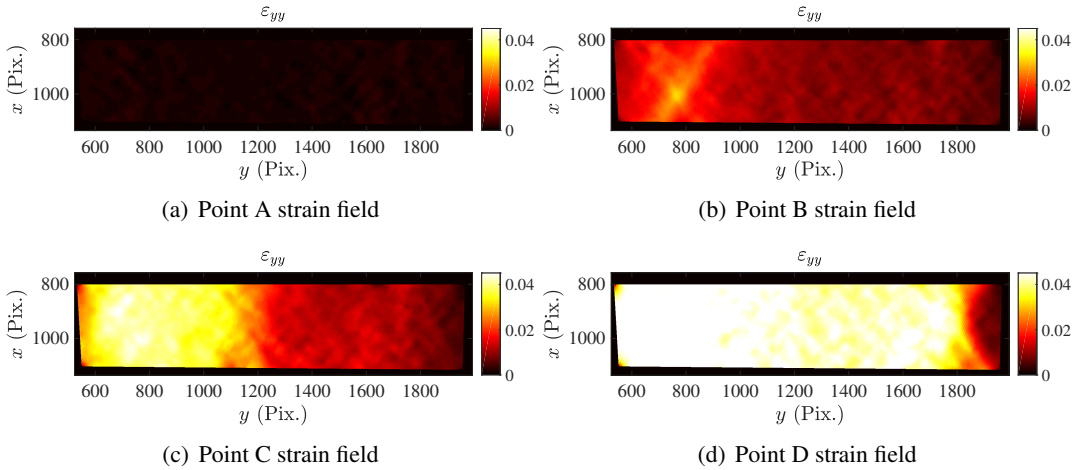

(a) Point A strain field

(b) Point B strain field

(c) Point C strain field

(d) Point D strain field

Figure 4: Evolution of the axial strain field during the loading

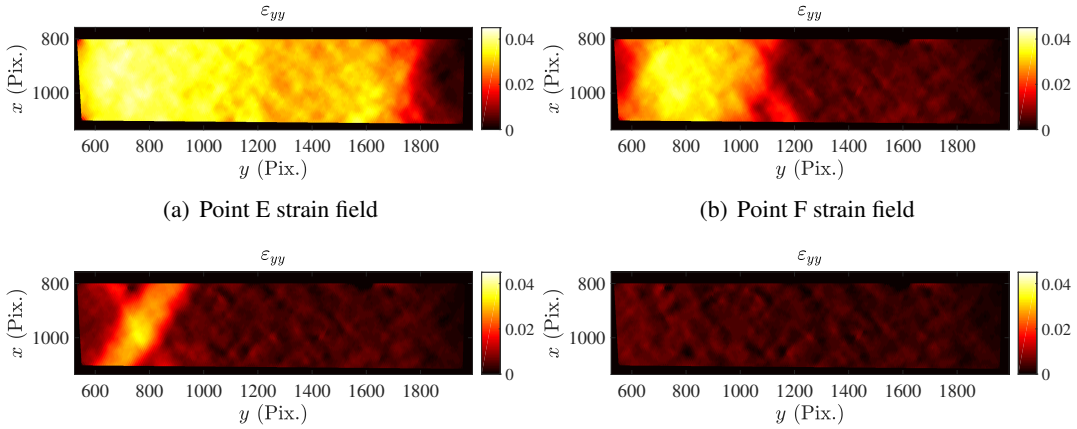

(a) Point E strain field

(b) Point F strain field

(c) Point G strain field

(d) Point H strain field

Figure 5: Evolution of the axial strain field during the unloading

4.2 Local stress-strain curve inside and outside localization bands

In this subsection, we aim to compare the 'local' and macro stress and strain curve. In order to obtain different evaluations of the axial strain, three gauges (see Figure 6) are considered:

Gauge 1 Local zone where the localization bands initiate;

Gauge 2 Global central zone;

Gauge 3 Local zone where the localization bands stop at the end of loading;

Thus it means that gauge 1 will remain mostly inside the transformation zone from the beginning of test. On the contrary gauge 3 will stay nearly outside the localization bands for the most of the time during loading and unloading. This differentiation in terms of strain value, helps us focusing on the difference of the mechanical property inside and outside the band.

As we can see in Figure 6 and Figure 7, 'local' behaviors (in gauge 1 and 3) of the NiTi 1Dstrip differ from the macroscopic behavior (gauge 2). Gauge 1 has the smallest stress threshold for phase transformation, meanwhile zone gauge 3 exhibits the highest stress threshold.

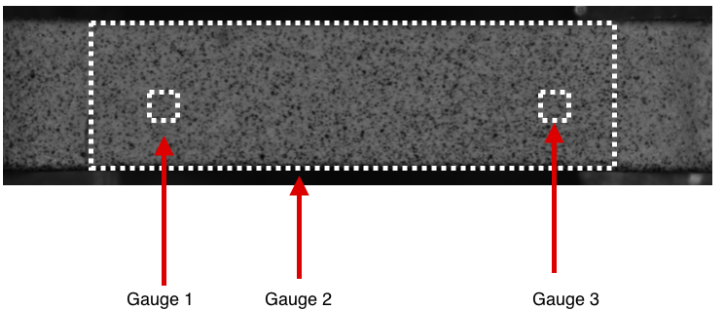

Figure 6: Three gauges of observation

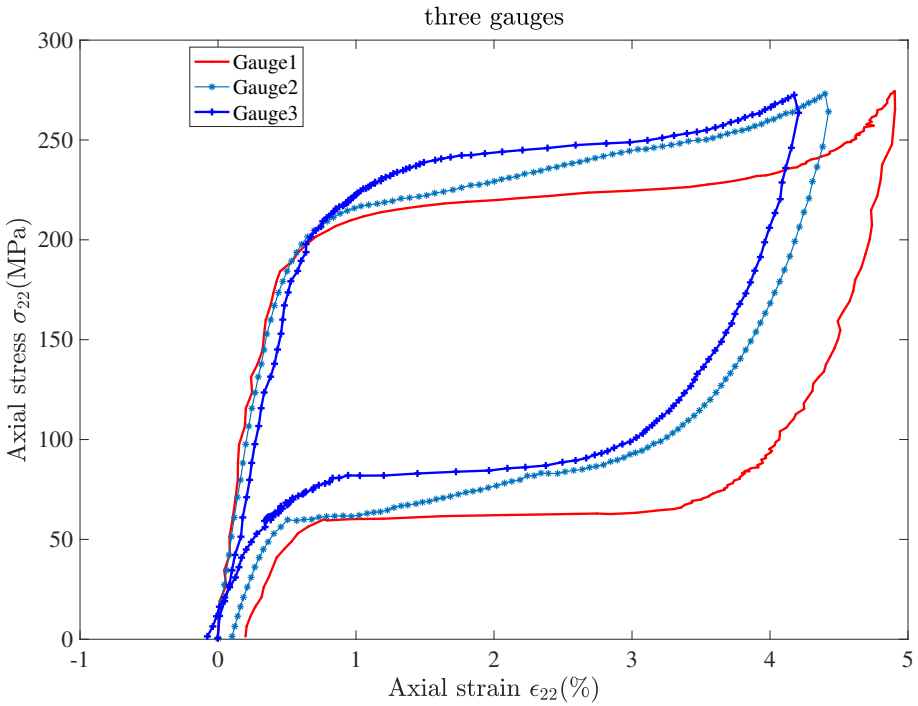

(a) Three different stress-strain curves for different gauge zones

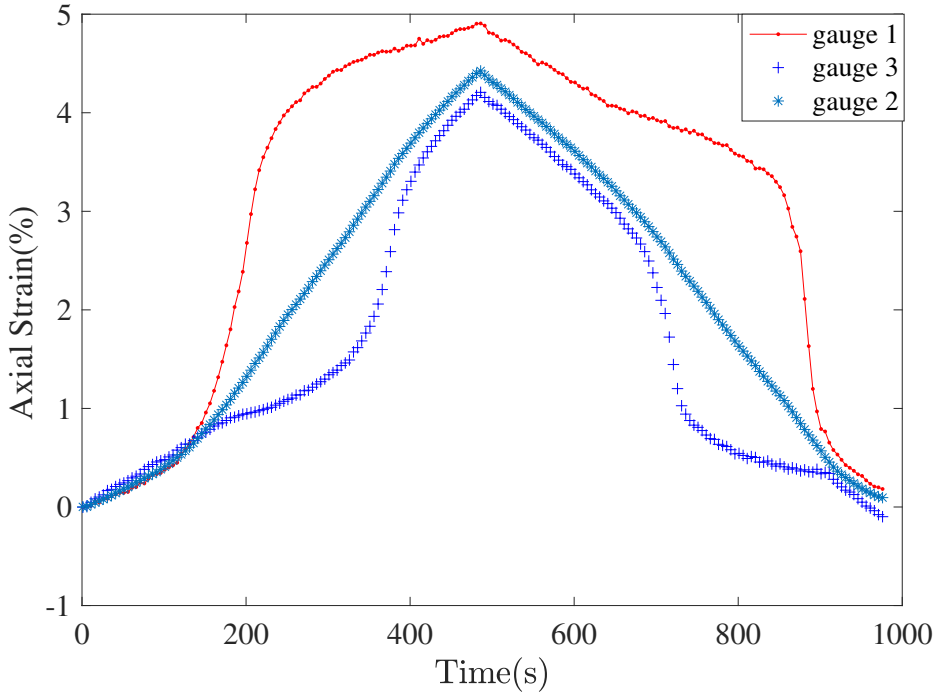

(b) Temporal evolution of the mean strain value based on different gauge

Figure 7: Comparison in three gauge

In order to better illustrate the spatial distribution of the strain field, the strain value along a specific line is plotted in Figure 8. The 4 different curves correspond to strain fields of Point A, B, C and D in Figure 3 and Figure 4. As we can see , even inside the localization bands (strain field of Point D in Figure 3), there is a relative strong fluctuation in terms of the axial strain value (up to 10% variation). The heterogeneous feature of strain field inside the localization bands should be the main reason of the maximum axial strain value difference in Figure 6. Two different hypotheses can be proposed to explain the difference observed in stress transformation threshold :

Local diffused martensite phase formed during the elastic regime For gauge 1, during the elastic regime, a small martensite phase amount seems to be created during the 'elastic' regime. A relatively lower germination energy may consequently be required to bypass the transformation threshold (by a reduction of surface tension). When the stress rises during the loading step, this zone is the first zone to fully transform from austenite to martensite. The localization bands begin to enlarge and propagate when the volume fraction of martensite is highly enough to equalize thermodynamic potential energy difference with other local zones. A combination of X-ray diffraction and Digital Images Correlation measurement may help to validate or invalidate this hypothesis. This work is in progress.

Structure effect As shown in Figure 8, the strain variation inside the localization bands remains relatively large. The difference in local and macroscopic behaviors could be the result of the combination of geometry effect (the smallest section is favored for nucleation - even considering a small geometrical defect) and heat conduction effect (temperature in zones aside the first nucleation area increases due to latent heat and conduction, even at small deformation rate). Implementation of the constitutive law in development inside a numerical modeling with implementation of geometry defect and heat equation resolution (including heat sources, conduction and convection) would help to validate or invalidate this hypothesis. This work is in progress.

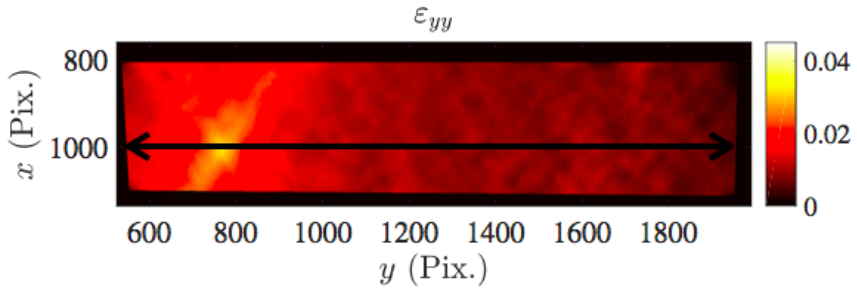

(a) Point B strain field along the chosen line

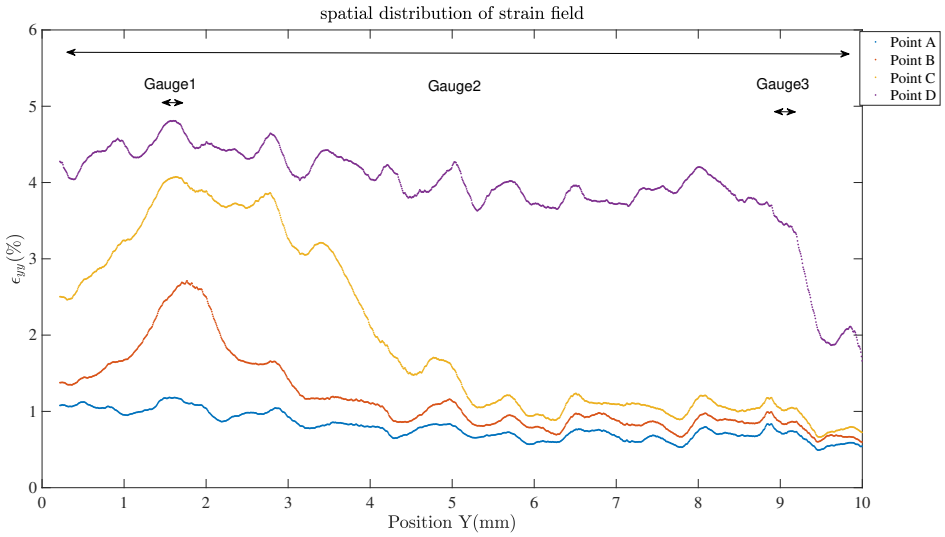

(b) Axial strain variation along the chosen line

Figure 8: Spatial evolution of the local strain value along the chosen line

5 Conclusions

The displacement-controlled uniaxial loading test over 1D strip of NiTi alloy helps us to understand the mechanical behavior of NiTi. DIC is a powerful tool which permits to capture the temporal evolution of the global strain field during the test, thus leading to a better understanding of the formation and propagation of the localization bands and hysteresis of NiTi alloy. By comparing the 'local' stress-strain curve for the zone inside and outside the localization, a difference of stress threshold in both loading and unloading is revealed. Local diffused martensite during the elastic regime, temperature changes due to the phase transformation and multi-axiality of stress may cause these types of stress threshold difference.
To fully understand the reason of this stress threshold difference, two new tests need to be considered : Firstly, a stereo-hybrid measurement (synchronized infrared and optic camera acquisition) would help us to capture both the temperature and strain field at the same time, which helps to verify whether the temperature change is involved in this difference of the stress threshold. Secondly, a combination of X-ray diffraction and digital images correlation would permit to measure the volume fraction of each phase in this type of gauge. Indeed, through spatial scan of X-ray spot in the central zone, marteniste phase's volume fraction distribution field can be related to the strain field calculated by DIC. Until now, we are still working in both directions.

References

[1] Lexcellent, C. and Blanc, P. Phase transformation yield surface determination for some shape memory alloy. *Acta mater.*, 52, No.8, pp. 2317-2324, 2004.

[2] He,Y. and Sun, Q. Rate-dependent domain spacing in a stretched strip *International Journal of Solid and Structure*, 47(20): 2775-2793, 2010.

[3] D. Depriester, A. Maynadier, K. Lavernhe-Taillard and O. Hubert. Thermomechanical modelling of a NiTi SMA sample submitted to displacement-controlled tensile test. *International Journal of Solids and Structures*, 51, 10 (2014) 1901-1922.

[4] T. Zvonimir, F. Hild and S. Roux. Mechanical-aided Digital Images Correlation. *Strain Analysis*, 48:330-343, 2013.

[5] M. Bertin, F. Hild, S. Roux, F. Mathieu, H. Leclerc, P. Aimedieu Integrated digital image correlation applied to elastoplastic identification in a biaxial experiment *J. Strain Analysis*, 2016, Vol. 51(2) 118-131.

[6] J.A.Shaw and S Kyriakides. On the nucleation and propagation of phase transformation fronts in a niti alloy. *Acta mater.*, 45, No.2, pp. 683-700, 1997.